Anatomical measurements correlate with individual magnetostimulation thresholds for kHz-range homogeneous magnetic fields

Omer Burak Demirel[a)]
Department of Electrical and Electronics Engineering, Bilkent University, Ankara 06800, Turkey
National Magnetic Resonance Research Center (UMRAM), Bilkent University, Ankara 06800, Turkey
Department of Electrical and Computer Engineering, University of Minnesota, Minneapolis, MN 55455, USA
Center for Magnetic Resonance Research, University of Minnesota, Minneapolis, MN 55455, USA

Toygan Kilic
Department of Electrical and Electronics Engineering, Bilkent University, Ankara 06800, Turkey
National Magnetic Resonance Research Center (UMRAM), Bilkent University, Ankara 06800, Turkey

Tolga Çukur and Emine Ulku Saritas
Department of Electrical and Electronics Engineering, Bilkent University, Ankara 06800, Turkey
National Magnetic Resonance Research Center (UMRAM), Bilkent University, Ankara 06800, Turkey
Neuroscience Program, Aysel Sabuncu Brain Research Center, Bilkent University, Ankara 06800, Turkey

(Received 4 September 2019; revised 6 January 2020; accepted for publication 13 January 2020; published 5 February 2020)

Purpose: Magnetostimulation, also known as peripheral nerve stimulation (PNS), is the dominant safety constraint in magnetic resonance imaging (MRI) for the gradient magnetic fields that operate around 0.1–1 kHz, and for the homogeneous drive field in magnetic particle imaging (MPI) that operates around 10–150 kHz. Previous studies did not report correlations between anatomical measures and magnetostimulation thresholds for the gradient magnetic fields in MRI. In contrast, a strong linear correlation was shown between the thresholds and the inverse of body part size in MPI. Yet, the effects of other anatomical measures on the thresholds for the drive field remain unexplored. Here, we investigate the effects of fat percentage on magnetostimulation thresholds for kHz-range homogeneous magnetic fields such as the drive field in MPI, with the ultimate goal of predicting subject-specific thresholds based on simple anatomical measures.
Methods: Human subject experiments were performed on the upper arms of 10 healthy male subjects (age: 26 ± 2 yr) to determine magnetostimulation thresholds. Experiments were repeated three times for each subject, with brief resting periods between repetitions. Using a solenoidal magnetostimulation coil, a homogeneous magnetic field at 25 kHz with 100 ms pulse duration was applied at 4-s intervals, while the subject reported stimulation via a mouse click. To determine the thresholds, individual subject responses were fitted to a cumulative distribution function modeled by a sigmoid curve. Next, anatomical images of the upper arms of the subjects were acquired on a 3 T MRI scanner. A two-point Dixon method was used to obtain separate images of water and fat tissues, from which several anatomical measures were derived: the effective outer radius of the upper arm, the effective inner radius (i.e., the muscle radius), and fat percentage. Pearson's correlation coefficient was used to assess the relationship between the threshold and anatomical measures. This statistical analysis was repeated after factoring out the expected effects of body part size. An updated model for threshold prediction is provided, where in addition to scaling in proportion with the inverse of the outer radius, the threshold has an affine dependence on fat percentage.
Results: A strong linear correlation ($r = 0.783$, $P < 0.008$) was found between magnetostimulation threshold and fat percentage, and the correlation became stronger after factoring out the effects of outer radius ($r = 0.839$, $P < 0.003$). While considering body part size alone did not explain any significant variance in measured thresholds ($P > 0.398$), the updated model that also incorporates fat percentage yielded substantially improved threshold predictions with $R^2 = 0.654$ ($P < 0.001$).
Conclusions: This work shows for the first time that fat percentage strongly correlates with magnetostimulation thresholds for kHz-range homogenous magnetic fields such as the drive field in MPI, and that the correlations get even stronger after factoring out the effects of body part size. These results have important practical implications for predicting subject-specific thresholds, which in turn can increase the performance of the drive field and improve image quality while remaining within the safety limits. [https://doi.org/10.1002/mp.14032]

Key words: anatomical measurements, magnetic particle imaging, magnetostimulation, peripheral nerve stimulation (PNS), threshold prediction

1. INTRODUCTION

Imaging modalities that utilize time-varying magnetic fields are subject to two fundamental safety constraints: peripheral nerve stimulation (PNS), also known as magnetostimulation, and specific absorption rate (SAR), also known as tissue heating. Numerous studies have been conducted to date to determine the safety limits in magnetic resonance imaging (MRI) for both gradient magnetic fields (operating around 100 Hz to 1 kHz) and radiofrequency (RF) magnetic fields (operating around 10 to 400 MHz).[1–3] It has been shown that PNS is the dominant safety constraint for gradient magnetic fields in MRI, with a typical dB/dt limit of 20 T/s,[4] whereas SAR is considered to be the main safety constraint for RF fields,[2] with a typical limit of 4 W/kg for whole body MRI.[4]

The drive field in magnetic particle imaging (MPI), on the other hand, operates at a different frequency range. In-house MPI scanners built in lab settings have drive field frequencies ranging between 10 and 150 kHz,[5–8] whereas the commercially available preclinical scanners operate at 25 and 45 kHz.[9,10] In this frequency range, the effects of the time-varying magnetic fields remain underinvestigated. Recent studies indicate that magnetostimulation is the main safety constraint on the drive field in MPI.[11–13] Magnetostimulation thresholds have been shown to decrease in a hyperbolic fashion as a function of frequency,[11] to decrease with increasing pulse duration and stabilize for pulses longer than 20 ms,[14] and to first decrease then increase with increasing duty cycle, reaching a peak value at 100% duty cycle.[15] Beyond MPI sequence parameters, thresholds have also been reported to strongly correlate with the inverse of the body part size that is exposed to the magnetic field.[11] This correlation also helps explain why transverse fields that create a bigger effective flux loop can have up to three times lower thresholds than axial fields.[12,16]

The aforementioned results are particularly important considering that the amplitude and frequency of the drive field directly affect signal-to-noise ratio, resolution, and scan time in MPI.[17] Therefore, to improve image quality while avoiding potential nerve stimulation, all factors that affect PNS must be well characterized. Considering the relatively large inter-subject variations in magnetostimulation thresholds, a potential question of interest is whether one can predict a subject-specific threshold given simple anatomical measurements. As mentioned above, the inverse of body part size is a primary factor that is strongly correlated with magnetostimulation thresholds in MPI.[11] In contrast, previous work on magnetostimulation in MRI did not show any correlation between body part size and thresholds. Furthermore, no significant correlation was reported between fat percentage or fat layer thickness and thresholds either.[18] This lack of correlations with anatomical measures can be due to the competing dependencies caused by the linear variation in the gradient magnetic field of MRI.[18] Hence, considering the differences in the types and frequencies of the applied fields, the effects of fat percentage on MPI magnetostimulation thresholds need to be examined independently. Quantifying these effects has the potential to help explain the large inter-subject variations in thresholds.

In this work, we systematically investigate the effects of fat percentage on magnetostimulation thresholds for kHz-range homogeneous magnetic fields, such as the drive field in MPI. We perform magnetostimulation experiments on the upper arms of 10 human subjects at 25 kHz, with additional fat percentage measurements of the same region using a 3 T MRI scanner. The results show for the first time that there is a strong linear correlation between fat percentage and magnetostimulation thresholds, and that this correlation gets stronger when the effect of the arm size is factored out. For threshold prediction, we provide an updated model that incorporates the effect of both the body part size and fat percentage. These results imply that simple anatomical measures can be utilized to predict subject-specific thresholds, which can in turn allow tuning of scanning parameters to improve scan efficiency in MPI.

2. MATERIALS AND METHODS

This study was approved by Bilkent University Ethics Committee. We designed and conducted human subject experiments with the goal of demonstrating the effects of fat/muscle content on magnetostimulation thresholds. A total of 10 healthy male subjects were recruited after being screened for safety considerations (e.g., presence of metallic implants, aneurysm clips, pacemakers, etc. in their body). The mean and standard deviations (SD) for the age, weight, and height of the subjects were 26 $\pm$ 2 yr, 82 $\pm$ 13 kg, and 181 $\pm$ 5 cm. Magnetostimulation thresholds were measured on the upper arms of the subjects. The effective radii of the mid-upper arms were 5.07 $\pm$ 0.44 cm (mean $\pm$ SD). Only one of the subjects was left-handed, and 50% of the subjects chose to place their dominant arms inside the magnetostimulation setup. The magnetostimulation experiments were repeated three times for each subject, with brief resting periods between repetitions. The subjects did not report any pain or discomfort. They described the sensations as a mild twitching or tingling at different locations on their upper arms, sometimes extending to their fingers. Next, MRI scans of the upper arms of the subjects were performed on a 3 T Siemens Magnetom Trio MRI scanner to quantitatively determine fat and muscle tissue contents.

2.A. Magnetostimulation experiments

Magnetostimulation thresholds were measured on the upper arms of the subjects using a solenoidal coil, as shown in Fig. 1. This coil generated an axial magnetic field, and had a free bore size of 11 cm in diameter and 17 cm in length. The magnetic field at the center of the bore had greater than 95% homogeneity in a 7 cm-long region. All experiments were conducted at a single frequency of 25 kHz. This frequency was chosen for three reasons: (a) 25 kHz is the most widely used frequency for the drive field in MPI. (b) Our previous work has shown that magnetostimulation thresholds

decrease with increasing frequency, nearly reaching an asymptotic value for frequencies higher than 20 kHz.[11] (c) Since 25 kHz is beyond the human hearing range, working at this frequency avoids audio feedback from the solenoidal coil that could otherwise cause false reporting of stimulation.[18,19] A pulse duration of 100 ms was chosen, based on our earlier results on pulse duration dependence of magnetostimulation limits, which showed that the thresholds stabilize for pulses longer than 20 ms.[14]

Figure 1 outlines the flow of the magnetostimulation experiments. The shapes and amplitudes of the magnetic pulses were controlled on a PC in MATLAB, and sent to a power amplifier via a data acquisition (DAQ) module. The solenoidal coil was impedance matched to the power amplifier at 25 kHz using a capacitive L-section circuit. During the experiments, the current through the coil was measured in real time using a Rogowski AC current probe via the DAQ module. Using the pre-measured solenoidal coil sensitivity of 410 μT/A, the corresponding magnetic field waveform and the peak-to-peak (pp) value of the applied field were computed. The maximum magnetic field that could be generated with this setup at 25 kHz was 72 mT-pp. Due to this hardware limitation, stimulation could only be induced on subjects with relatively large arms.

The subjects placed their arm inside the solenoidal coil and were instructed to click a mouse button when they feel a nerve stimulation sensation. During the experiments, the magnetic pulses were applied at 4-s intervals to wait for a potential "mouse click" feedback and to avoid numbing the nerves. Each experiment consisted of 3 stages. In the first stage, an initial rough estimate of the magnetostimulation threshold, $B_{th,1}$, was obtained by increasing the pulse amplitude gradually until the subject reported a stimulation. In the second stage, the pulse amplitudes were randomly varied within ±15% of $B_{th,1}$ with a step size of 5% of $B_{th,1}$ to obtain a more accurate estimate of the threshold, $B_{th,2}$. In the last stage, the pulse amplitudes were randomly varied within ±15% of $B_{th,2}$ with a finer step size of 1% of $B_{th,2}$ to arrive at a final high accuracy estimate of the threshold value, B_{th}. Note that the second and third parts of the experiment utilized random ordering of the pulse amplitudes to avoid ordering-induced bias and psychophysical hysteresis effects.[11] Each experiment lasted around 3 min. At the end of the experiment, the subject was asked to remove their arm from the solenoidal coil. Following a few minutes of resting period, the entire experiment was repeated with the same arm of the subject placed in approximately the same position in the coil. In total, the experiments were repeated three times for each subject to determine intra-subject variations.

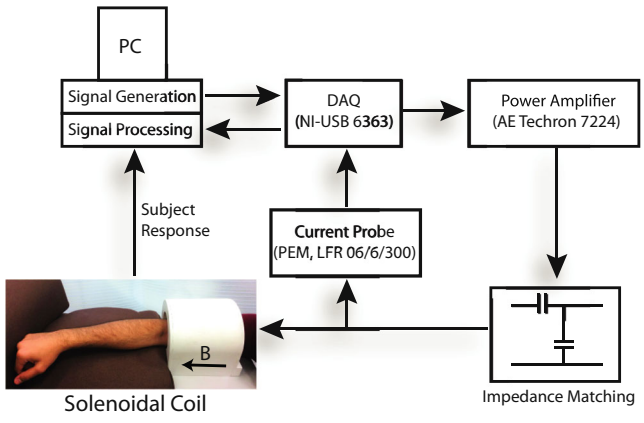

FIG. 1. Flowchart of the magnetostimulation experiments conducted in the upper arm at 25 kHz. A solenoidal coil with 11 cm diameter and greater than 95% homogeneity in a 7cm-long region was utilized, generating an axial magnetic field (direction shown with a black arrow in the photo). Pulse shapes and amplitudes were controlled using a PC and a data acquisition (DAQ) module. The subjects reported stimulation response via a mouse click, which was then used to determine the subsequent pulse amplitudes. A current probe was used for real-time measurement of the magnetic field in the coil. [Color figure can be viewed at wileyonlinelibrary.com]

2.B. Magnetostimulation data analysis

Subject responses from the second and third stages of a given experiment (i.e., the stages with randomized pulse amplitudes) were merged for analysis. Example stimulation response data are plotted in Fig. 2, where "1" and "0" denote that the subject reported a stimulation or remained unresponsive, respectively. Next, the magnetostimulation threshold was modeled as a probabilistic event, with a cumulative distribution function (CDF) given by a sigmoid curve[11,14,15]:

$$F(B) = \left(1 + e^{\frac{-(B-B_{th})}{W}}\right)^{-1} \quad (1)$$

Here, B (mT-pp) is the measured magnetic field strength, B_{th} (mT-pp) is the magnetostimulation threshold (i.e., the 50% crossing of the sigmoid curve), and W (mT-pp) is the transition width. In this model, a non-zero W allows for inconsistencies in stimulation response data [see Fig. 2(b)]. To determine B_{th} and W, subject responses were fitted to Eq. (1) using least-squares regression. This fitting procedure was performed separately for each experiment of each subject.

2.C. MRI experiments

Magnetic resonance imaging experiments were performed on a 3T Siemens Magnetom Trio MRI scanner using an 8-channel spine matrix coil. Subjects were placed in the scanner in head-first prone position, with one arm (the one that was placed in the solenoidal coil) extended over their heads. Majority of the subjects had reported feeling the stimulation sensation on their mid-upper arms. To help localize this region during imaging, a fiducial marker (a vitamin E capsule) was placed a few cm away from the mid-upper arm area. A two-point Dixon method was used to obtain separate images of water and fat tissues from axial slices in the mid-upper arm region.[20,21] The imaging parameters were: TR = 5.27 ms, TE_1 = 2.45 ms, TE_2 = 3.675 ms, flip angle = 9°, FOV = 380 × 285 mm^2, matrix size = 320 × 240, with 32 s total scan time.

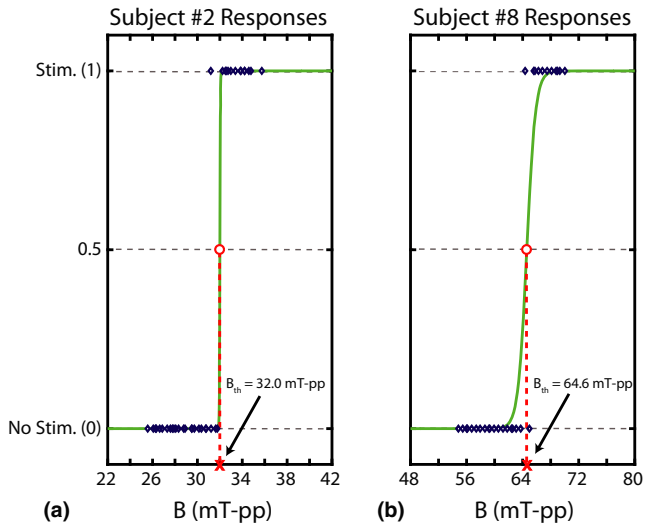

FIG. 2. Example stimulation response data. Blue diamonds represent the subject responses, with "1" denoting that the subject reported a stimulation sensation and "0" denoting that the subject remained unresponsive. The green curves represent fitted sigmoid functions, and red circles denote the estimated magnetostimulation thresholds (i.e., 50% crossing levels). (a) Example of a sharp transition (W = 0.011 mT-pp) with B_{th} = 32.0 mT-pp from Subject #2, and (b) example of a wider transition (W = 0.308 mT-pp) with B_{th} = 64.6 mT-pp from Subject #8. Although these two subjects had similar arm sizes (r_{out} = 5.14 cm for Subject #2 vs r_{out} = 5.55 cm for Subject #8), their magnetostimulation thresholds are very different. [Color figure can be viewed at wileyonlinelibrary.com]

2.D. MRI Image analysis

As visually outlined in Fig. 3, fat tissue and water tissue images were processed in MATLAB to obtain four different anatomical measures. First, matching regions of interest (ROI) were manually selected on both the water and fat images for a given subject. This ROI selection removed the fiducial marker and any other unrelated anatomical parts from consideration. Next, the water and fat images were individually normalized by their respective maximum pixel intensities. A Canny edge detection algorithm was applied to the fat image to determine the inner and outer edges of the subcutaneous fat region (labeled as "inner ring" and "outer ring" in Fig. 3). The interior regions of the rings were filled via a flood-fill operation to create two binary masks, labeled as "filled inner ring" and "filled outer ring" in Fig. 3.

Next, the effective radii of the two rings, r_{in} and r_{out}, were calculated. For the smooth outer ring, r_{out} was computed as the circumference of the filled ring divided by 2π. Due to the folded nature of the inner ring, r_{in} was computed as the mean distance between the points on the ring and the center of mass of the filled ring. Note that r_{out} is the actual effective radius of the mid-upper arm of a subject, which could easily be calculated by measuring the circumference via a measuring tape, without necessitating an MRI scan. On the other hand, r_{in} can be considered as the effective radius for the muscle tissue, and measuring this parameter requires imaging of the anatomy.

In addition, the fat percentage was calculated from the MRI images using two different approaches. In the first approach, the fat percentage was calculated directly from the fat and water images, that is,

$$Fat\%_{direct} = \frac{\sum_{m=1}^{M}\sum_{n=1}^{N} I_F(m,n)}{\sum_{m=1}^{M}\sum_{n=1}^{N}(I_F(m,n)+I_W(m,n))} \times 100 \tag{2}$$

where I_F and I_W are the normalized fat image and the normalized water image, respectively, and the images are of size $M \times N$. Here, the initial individual normalization of the images ensures that the pixel intensities are not biased by T_1, T_2, or proton density contrast differences between the two tissue types. However, each MRI image still experiences a shading effect due to spatial variations in receive coil sensitivities. Therefore, in the second approach, binary masks of the fat and water tissues were first extracted to remove any shading. The filled inner ring was considered as the binary mask of the water tissue. A binary mask of the fat tissue was then computed as the difference of the filled outer ring and the filled inner ring images (see Fig. 3). The resulting fat percentage, $Fat\%_{binary}$, was then calculated using the binary masks of fat and water as I_F and I_W in Eq. (2), respectively.

2.E. Proposed model for predicting magnetostimulation thresholds

One of the goals of this work is to determine whether the considered anatomical measures would allow for accurate prediction of subject-specific magnetostimulation thresholds. Our previous work had shown a strong linear relation between r_{out}^{-1} and B_{th}, leading to the following original model:

$$B_{th} = \frac{\lambda_{fit}}{r_{out}} \tag{3}$$

Here, λ_{fit} = 285 mT-pp · cm was fitted using the combined magnetostimulation results from the lower arm and lower leg.[11] In this work, we suggest that incorporating the effects of fat percentage can improve threshold predictions. Accordingly, we propose the following model, featuring an affine adjustment to Eq. (3):

$$B_{th} = \frac{\lambda_{fit}}{r_{out}}\left(1 + m_{fit}\frac{Fat\% - F_{fit}}{100}\right) \tag{4}$$

In this updated model, r_{out} and $Fat\%$ denote the anatomical measurements from the subject, and λ_{fit}, m_{fit}, and F_{fit} are model parameters to be determined via regression. Note that when $F_{fit} = Fat\%$, this model simplifies to that in Eq. (3).

2.F. Statistical analysis

As a primary analysis, Pearson correlation coefficient was measured to identify linear relationships between magnetostimulation threshold and anatomical measures. Specifically, correlation coefficients were measured for the inverses

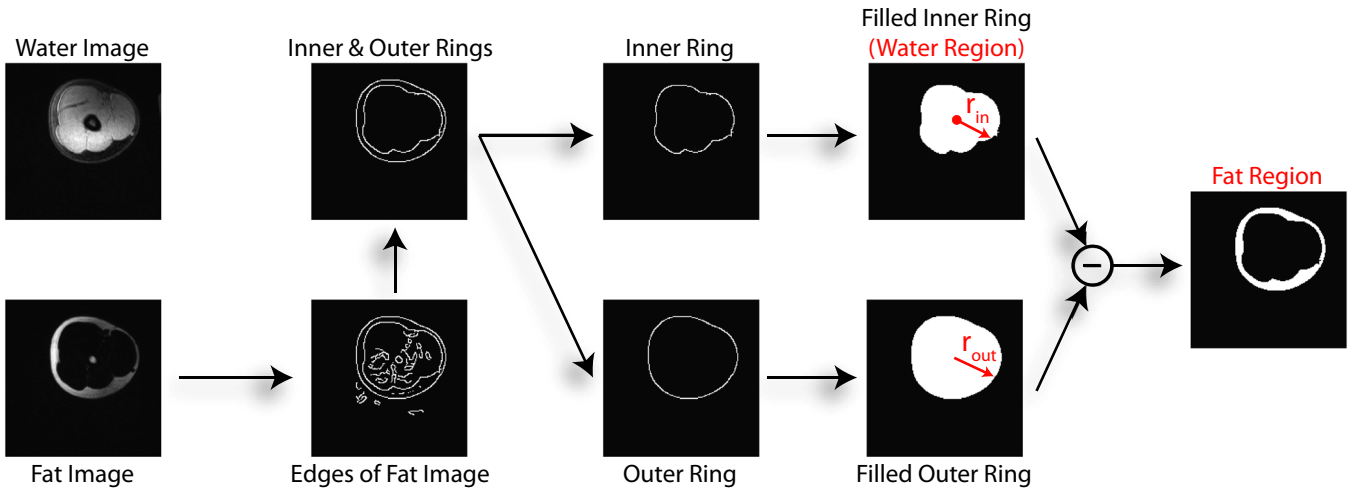

FIG. 3. Flowchart for obtaining 4 different anatomical measures from the MRI images. Example fat and water images from the mid-upper arm region of Subject #1 are shown. A Canny edge detection algorithm was used to extract the edge information from the fat image, followed by the isolation of the inner and outer rings of the subcutaneous fat region. The effective radius of the outer ring (r_{out}) was calculated as the circumference of the filled outer ring divided by 2π. The effective radius of the inner ring (r_{in}) was calculated as the mean distance between the points on the ring and the center of mass of the filled ring (shown with red dot). The filled inner ring was considered as the binary mask for water tissue (i.e., muscle), and the difference between the filled outer ring and the filled inner ring was used as the binary mask for fat tissue. A direct fat percentage, Fat% $_{direct}$, was computed from the summed normalized pixel intensities of the fat image and the water image. In addition, Fat% $_{binary}$ was computed from the summed binary masks. [Color figure can be viewed at wileyonlinelibrary.com]

of the radii (i.e., r_{in}^{-1} and r_{out}^{-1}) and B_{th}, $Fat\%_{direct}$ and B_{th}, and $Fat\%_{binary}$ and B_{th}.

Next, a secondary analysis was performed to investigate the trends in the deviations from the expected value of magnetostimulation threshold given body part size. Using Eq. (3), we calculated the expected threshold, $B_{exp,}$, for a given r_{out}. To factor out the effect of radius from B_{th}, the ratio of measured threshold to expected threshold was calculated as B_{th}/B_{exp}. Finally, Pearson correlation coefficient was utilized to evaluate the linear relationships between the four anatomical measures and B_{th}/B_{exp}.

Finally, to test whether the considered anatomical measures allow for a subject-specific prediction of magnetostimulation thresholds, B_{th} measurements were predicted using both the original model in Eq. (3) and the updated model in Eq. (4). For these two models, the significance of the coefficient of determination, R^2, was determined via an F test.

3. RESULTS

3.A. Magnetostimulation thresholds

Figure 4(a) shows the magnetostimulation thresholds for all 3 repetitions from all 10 subjects, that is, a total of 30 experiments. As illustrated in Fig. 4(a), there is broad inter-subject variation in threshold values. The mean threshold across all experiments was 50.6 mT-pp, with a maximum deviation of 44% from this mean value. The intra-subject variation was relatively small, and ranged between a maximum deviation of 0.77% and 8.38% from the mean values. This small variation indicates a high degree of consistency and repeatability in subject responses. For the remainder of the analysis, the average of three repetitions was taken as the magnetostimulation threshold of each subject.

3.B. Correlations with anatomical measures

Figure 5 shows the scatter plots of the magnetostimulation thresholds for all 10 subjects as functions of the four anatomical measures extracted from the MRI images: r_{out}^{-1}, r_{in}^{-1}, $Fat\%_{direct}$, and $Fat\%_{binary}$. Since our hardware limitations restricted the range of distributions in upper arm sizes, r_{out} had a mere 15% maximum deviation around a mean value of 5.07 cm. Likewise, r_{in} had a 17% maximum deviation around a mean value of 4.07 cm. Note that this restriction did not

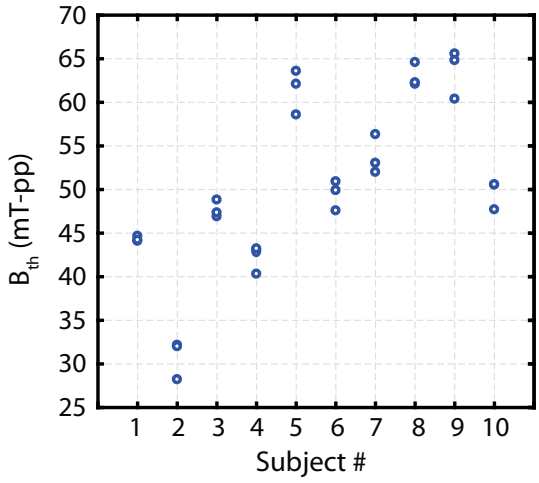

FIG. 4. Results of the magnetostimulation experiments in the upper arm at 25 kHz, showing magnetostimulation thresholds for all 3 repetitions from all 10 subjects. The mean threshold across all experiments was 50.6 mT-pp with a maximum deviation of 44%, showing a broad inter-subject variation. The intra-subject variation was relatively limited, ranging between a maximum deviation of 0.77% (for Subject #1) and 8.38% (for Subject #2) from the mean values. [Color figure can be viewed at wileyonlinelibrary.com]

pose a limitation for the purposes of this work, as a wide distribution in fat percentage was still achieved: $Fat\%_{direct}$ displayed 35% maximum deviation around a mean value of 32, and $Fat\%_{binary}$ displayed 41% maximum deviation around a mean value of 32.

Figure 5(a) clearly demonstrates that subjects with very similar arm sizes can have considerably different threshold values. For example, Subject #2 has $r_{out}^{-1} = 0.19$ cm^{-1} with $B_{th} = 30.8$ mT-pp, whereas Subject #8 has $r_{out}^{-1} = 0.18$ cm^{-1} with $B_{th} = 63.0$ mT-pp. A linear fit was performed on each scatter plot, shown with red lines. Considering the theoretical model for the magnetostimulation thresholds as well as our earlier experimental results,[11] the linear fits for inverse radius vs B_{th} curves were forced to pass through the origin (i.e., B_{th} is expected to converge to zero as the effective radius approaches infinity). On the other hand, a non-zero y-intercept was allowed for the linear fits for fat percentage vs B_{th} curves (i.e., even if a person has zero fat, the remaining tissues would cause non-zero B_{th}). To assess the linear relationship between each anatomical measure and the magnetostimulation thresholds, Pearson correlation coefficient was computed. No significant correlation was observed between r_{out}^{-1} and B_{th} (r = 0.145, $P > 0.690$). While this result may seem to contradict our earlier work,[11] it was expected considering the narrow distribution in arm sizes imposed by hardware limitations. In contrast, a strong correlation was found between r_{in}^{-1} and B_{th} (r = 0.655, $P < 0.041$) despite the narrow distribution in r_{in}. Consistent with the hypothesis that fat content influences stimulation threshold, there were strong correlations between $Fat\%_{direct}$ and B_{th} (r = 0.783, $P < 0.008$), and between $Fat\%_{binary}$ and B_{th} (r = 0.747, $P < 0.014$).

3.C. Correlations after factoring out body part size

The previous analyses on correlation coefficients suggest strong linear relationship between B_{th} and fat percentage. Yet, variations in body part size may have confounded these analyses. To increase sensitivity in correlation analyses, the expected effects of the outer radius were factored out as described in Section 2.E. First, the expected thresholds for given r_{out} values were computed according to the original model in Eq. (3) with $\lambda_{fit} = 285$ mT-pp · cm.[11] These expected thresholds, B_{exp}, are shown with the black dashed line in Fig. 5(a). Then, the ratio of the measured threshold to expected threshold, B_{th}/B_{exp}, was computed for all subjects. In Fig. 6, the resulting B_{th}/B_{exp} values are plotted as functions of the four anatomical measures. For each subfigure, the red line denotes the linear fit with non-zero y-intercept. As seen in these plots, B_{th}/B_{exp} varies between 0.58 and 1.22, demonstrating a considerable range of deviation from the expected thresholds. Visually comparing Fig. 5(a) with Fig. 6(c) [or Fig. 6(d)], one can see that fat percentage can broadly account for these deviations.

Next, Pearson correlation coefficient was computed between each anatomical measure and B_{th}/B_{exp}, to assess how well each anatomical measure correlates with the deviation from the expected threshold. As expected, there was no significant correlation between r_{out}^{-1} and B_{th}/B_{exp} (r = −0.270, $P > 0.449$). Furthermore, there was no significant correlation between r_{in}^{-1} and B_{th}/B_{exp} (r = 0.328, $P > 0.355$). In contrast, the linear correlation with fat percentage was stronger after factoring out the effects of the outer radius. Accordingly, there were very strong correlations between $Fat\%_{direct}$ and B_{th}/B_{exp} (r = 0.839, $P < 0.003$), and between $Fat\%_{binary}$ and B_{th}/B_{exp} (r = 0.801, $P < 0.006$). These results indicate that fat content can explain variability in magnetostimulation thresholds even after accounting for variability that can be attributed to body part size.

3.D. Threshold predictions

The results in Fig. 6 suggest that we can improve threshold predictions by incorporating the effects of fat percentage via an affine adjustment to Eq. (3), as presented with the updated model in Eq. (4). For this updated model, keeping $\lambda_{fit} = 285$ mT-pp · cm as before[11] and using $Fat\%_{direct}$ during regression yields $m_{fit} = 2.27$ and $F_{fit} = 36.6$. Using $Fat\%_{binary}$ instead yields $m_{fit} = 1.74$ and $F_{fit} = 38.0$.

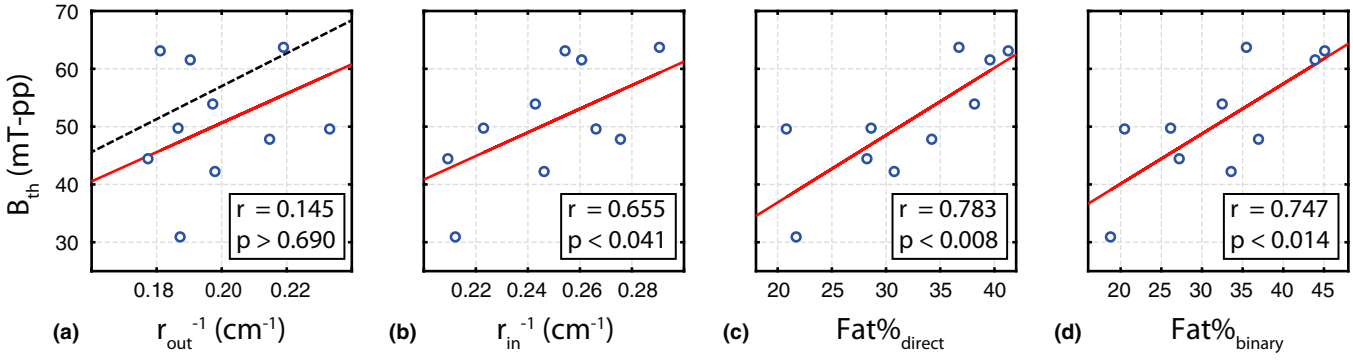

FIG. 5. Magnetostimulation thresholds from all 10 subjects, plotted as functions of the four anatomical measures extracted from the magnetic resonance images. The red lines show the linear fits to data points. (a) No significant correlation was found between the inverse of the outer radius and B_{th} (r = 0.145, $P > 0.690$). The black dashed line shows the expected thresholds based on Eq. (3). (b) A strong correlation was found between the inverse of the inner radius and B_{th} (r = 0.655, $P < 0.041$). Similarly, there were strong correlations (c) between $Fat\%_{direct}$ and B_{th} (r = 0.783, $P < 0.008$), and (d) between $Fat\%_{binary}$ and B_{th} (r = 0.747, $P < 0.014$). [Color figure can be viewed at wileyonlinelibrary.com]

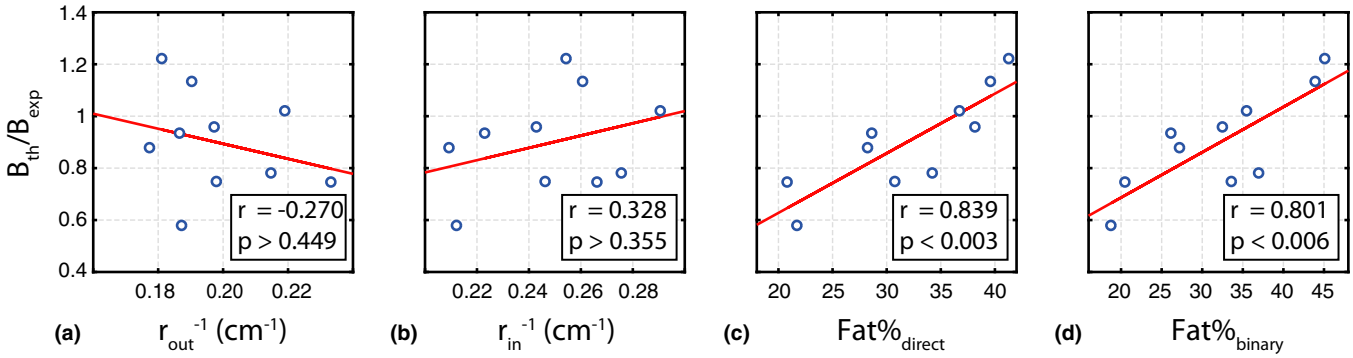

FIG. 6. Ratio of the measured magnetostimulation threshold to expected threshold computed using the original model in Eq. (3), factoring out the expected effects of the outer radius. The ratios for all 10 subjects are plotted as functions of the four anatomical measures extracted from the magnetic resonance images. The red lines show the linear fits to data points. No significant correlation was found (a) between the inverse of the outer radius and B_{th}/B_{exp} ($r = -0.270$, $P > 0.449$), and (b) between the inverse of the inner radius and B_{th}/B_{exp} ($r = 0.328$, $P > 0.355$). There were very strong correlations (c) between $Fat\%_{direct}$ and B_{th}/B_{exp} ($r = 0.839$, $P < 0.003$), and (d) between $Fat\%_{binary}$ and B_{th}/B_{exp} ($r = 0.801$, $P < 0.006$). [Color figure can be viewed at wileyonlinelibrary.com]

Figure 7 compares threshold prediction performances of the models in Eqs. (3) and (4). The original model in Eq. (3) that only considers body part size does not explain any significant variance in measured thresholds ($P > 0.398$). On the other hand, the updated model yields substantially improved predictions for B_{th}. Using $Fat\%_{direct}$ yields a coefficient of determination equal to $R^2 = 0.654$ ($P < 0.001$), whereas using $Fat\%_{binary}$ yields $R^2 = 0.581$ ($P < 0.017$). These results clearly suggest that subject-specific variability in stimulation thresholds can be predicted by using simple anatomical measures including body part size and fat percentage.

4. DISCUSSION

The human subject experiments in this work have shown strong correlations between fat percentage and magnetostimulation thresholds. The correlations with fat percentage became stronger when the effects of body part size were factored out, leading to the updated magnetostimulation model in Eq. (4). A previous study had also reported an anecdotal observation that the subjects with below average body fat tended to have lower thresholds in MRI.[18] However, no correlation between fat percentage or fat layer thickness and thresholds was found across a pool of 17 subjects. Moreover, that study did not find any correlation between body part size and thresholds, either. Our updated model in Eq. (4) offers an explanation to these seemingly contradicting results: fat percentage and body part size can have competing effects on magnetostimulation thresholds. Therefore, depending on the distribution of these two parameters for a group of subjects, it may be difficult to observe a correlation with any single one of the two parameters. In the current work, our hardware limitations restricted the range of distributions in upper arm sizes, whereas a relatively wide spread in fat percentage was still achieved. These conditions facilitated the observation of the correlation between fat percentage and thresholds, and allowed for the construction of the updated model in Eq. (4).

Other reasons for the discrepancy between our results and those of the aforementioned study[18] could be the differences in the types and frequencies of the applied magnetic fields. In MRI, gradient magnetic fields are spatially linear fields that operate around 100 Hz to 1 kHz. Particularly, the linear variation in the magnetic field can cause competing dependencies with respect to body part size or other anatomical measures.[18]

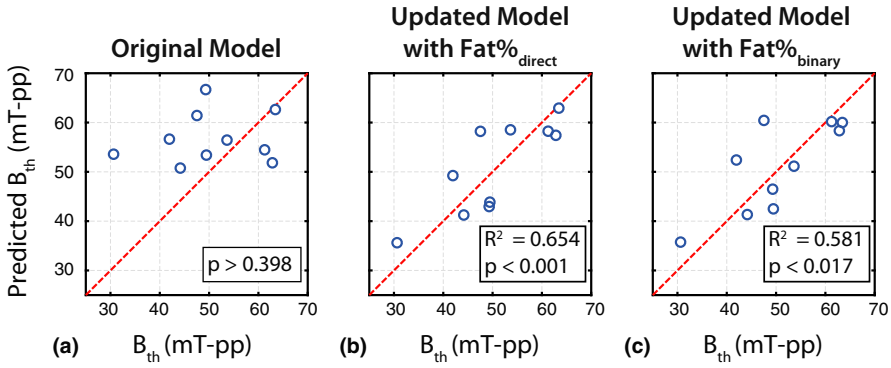

FIG. 7. Measured magnetostimulation thresholds vs predicted thresholds. (a) The original model in Eq. (3) only considers body part size and does not explain any significant variance in measured thresholds ($P > 0.398$). (b)–(c) The updated model in Eq. (4) yields substantially improved predictions by incorporating the effect of fat percentage, with $R^2 = 0.654$ ($P < 0.001$) using $Fat\%_{direct}$ and $R^2 = 0.581$ ($P < 0.017$) using $Fat\%_{binary}$. The red dashed lines show y = x. [Color figure can be viewed at wileyonlinelibrary.com]

In contrast, our magnetostimulation experiments for the drive field in MPI utilized spatially homogeneous magnetic fields at 25 kHz. In addition, according to the fundamental law of magnetostimulation,[3] magnetostimulation thresholds decrease with increasing frequency and reach an asymptote at high frequencies. We have previously shown that, for the drive field in MPI, B_{th} converges to its asymptotic value for frequencies higher than 20 kHz.[11] In the current study, operating in the asymptotic range may have also rendered it easier to observe correlations with anatomical measures.

In the updated model in Eq. (4), B_{th} scales directly in proportion with r_{out}^{-1} and affinely with respect to $Fat\%$. Thus, r_{out} is the primary factor in B_{th}, whereas $Fat\%$ has a secondary adjustment effect. For this reason, when a group of subjects has broadly distributed r_{out} and $Fat\%$ values, one should still be able to observe the linear correlation between r_{out}^{-1} and B_{th}. This is confirmed in our previous work that pooled threshold measurements from lower arms and lower legs of human subjects to achieve a broader distribution in effective radius[11]: 34% maximum deviation around a mean value of 4.87 cm. The nature of this pooled dataset likely increased sensitivity in detecting correlation with body part size despite the unaccounted variations in fat percentage (which were not measured at the time).

The updated model contains three free parameters, whereas the original model contained a single parameter. A more complex model naturally has improved potential to account for variability in the data. Note, however, that the proposed model is physiologically motivated: the mechanism for the observed fat percentage dependence of magnetostimulation thresholds could be the relative positioning of the conductive muscle tissue with respect to the stimulated peripheral nerves, which are mostly located within the skin layer. Conductive materials that are subjected to time-varying magnetic fields are known to cause a decrease in their internal electric field and a localized increase in the electric field exterior to the material. Therefore, a lower fat percentage (i.e., a thinner fat layer) may position the peripheral nerves closer to the muscle tissue, causing them to experience a higher electric field,[18] which in turn would cause a reduction in B_{th}. A recent electromagnetic simulation study on predicting PNS limits has also shown that electric field hotspots corresponded to regions of low-conductivity fat tissue positioned near a high-conductivity tissue such as muscle,[22] providing support for the abovementioned hypothesis and for the updated model in Eq. (4).

Similar to the case of r_{out} values, r_{in} values for the subjects in this work also had a relatively narrow distribution. Still, a strong linear correlation was found between r_{in}^{-1} and B_{th}. This result implies that the effective radius of the conductive muscle tissue has a dominant effect on B_{th}, as well as the proximity of the peripheral nerves to the muscle tissue as explained above. Nevertheless, measuring r_{in} requires imaging of the anatomy, which may not be practical in general.

A potential practical measure for categorizing body fat is the body mass index (BMI). For the recruited subjects in this work, BMI varied between 25.0 ± 2.9 kg/m^2 (mean ± SD). There was no significant correlation between BMI and B_{th} ($r = 0.325$, $P > 0.361$), whereas a relatively strong correlation was found between BMI and B_{th}/B_{exp} ($r = 0.638$, $P < 0.048$). However, for certain subjects, there were large deviations (as large as 58%) from the linear fit between BMI and B_{th}/B_{exp} (results not shown). Such large deviations are to be expected, since BMI is known to be an unreliable measure of body fat.[23] Body mass index tends to overestimate body fat for people with high muscle mass, and underestimate it for older people with low muscle mass. Therefore, as practical as BMI is, it is not a suitable anatomical measure for predicting B_{th}.

In this work, due to hardware limitation of the magnetostimulation setup, stimulation could only be induced on subjects with relatively large arms, all of which were male. Apart from this limitation and the initial screening for safety considerations, the subjects were recruited without any restrictions on age (as long as they were between ages 18–65 according to our ethics approval), height, or weight. Although female subjects were not recruited due to their relatively small arms, we do not expect any gender differences in the effects of anatomical measures described in this work. It should be noted that some of the previous clinical investigations of PNS in MRI were conducted on a much larger cohort of subjects, with $N > 150$.[24,25] In addition to these large-scale studies, coil-specific PNS experiments were conducted with N = 20–24 to investigate the thresholds for various types and sizes of gradient coils.[26,27] Similar to our work, there has also been PNS studies with a relatively small cohort of subjects (N = 5–10) to investigate the PNS thresholds for custom gradient systems in MRI, such as head-only or neck-insert gradient systems.[28,29] Further validation of the updated model in Eq. (4) on a larger cohort of subjects (with a balanced gender distribution and wider age range) would be beneficial to improve the statistical power of the analysis. Validating the model on different body parts (e.g., leg, torso) remains a future work, as well.

The results of this work have important practical implications for determining subject-specific thresholds to enable high efficiency scans. The twofold variation between the minimum and maximum threshold values in this work suggests at least a twofold variation in MPI scan efficiency if one operates at individual magnetostimulation thresholds. As a first step to determine these thresholds, one can easily compute the effective outer radius of a body part by measuring the circumference via a measuring tape. While using an MRI scanner for fat percentage measurements may be excessive in most cases, this parameter could alternatively be measured via much simpler devices such as a skinfold caliper or bioelectrical impedance analysis. Considering the different values for m_{fit} and F_{fit} produced by $Fat\%_{direct}$ and $Fat\%_{binary}$ measures, it remains to be shown how the parameters in Eq. 4 need to be adjusted when using a different device to measure fat percentage.

5. CONCLUSIONS

We have shown for the first time that fat percentage strongly correlates with magnetostimulation thresholds for kHz-range homogeneous magnetic fields such as the drive field in MPI, and that the correlations get even stronger after factoring out the effects of body part size. According to the updated model that we present, the thresholds scale proportionally with the inverse of body part size, and affinely with fat percentage. These results have important practical implications for predicting subject-specific thresholds from simple anatomical measures, which can enable MPI to operate at a higher drive field performance while avoiding magnetostimulation.

ACKNOWLEDGMENTS

This work was supported by the Turkish Academy of Sciences through TUBA-GEBIP 2015 program, and by the Science Academy, Turkey through BAGEP 2016 award.

CONFLICT OF INTEREST

The authors have no conflict to disclose.

[a]Author to whom correspondence should be addressed. Electronic mail: demirel@ee.bilkent.edu.tr.

REFERENCES

1. Reilly JP. Peripheral nerve stimulation by induced electric currents: exposure to time-varying magnetic fields. *Med Biol Eng Comput*. 1989;27:101–110.
2. Bottomley PA, Edelstein WA. Power deposition in whole-body NMR imaging. *Med Phys*. 1981;8:510–512.
3. Irnich W, Schmitt F. Magnetostimulation in MRI. *Magn Reson Med*. 1995;33:619–623.
4. ICNIRP. Medical magnetic resonance (MR) prodecures: protection of patients. *Health Phys*. 2004;87:197–216.
5. Muslu Y, Utkur M, Demirel OB, Saritas EU. Calibration-free relaxation-based multi-color magnetic particle imaging. *IEEE Trans Med Imaging*. 2018;37:1920–1931.
6. Sattel TF, Woywode O, Weizenecker J, Rahmer J, Gleich B, Borgert J. Setup and validation of an MPI signal chain for a drive field frequency of 150 kHz. *IEEE Trans Magn*. 2015;51:1–3.
7. Vogel P, Ruckert MA, Klauer P, Kullmann WH, Jakob PM, Behr VC. Traveling wave magnetic particle imaging. *IEEE Trans Med Imaging*. 2014;33:400–407.
8. Goodwill PW, Lu K, Zheng B, Conolly SM. An x-space magnetic particle imaging scanner. *Rev Sci Instrum*. 2012;83:033708.
9. MPI - Bruker's revolutionary modality for preclinical imaging. Bruker Biospin. https://www.bruker.com/fileadmin/user_upload/8-PDF-Docs/PreclinicalImaging/Brochures/MPI-PreClinical-Brochure.pdf. Accessed August 7, 2019.
10. MOMENTUM™ Imager | Magnetic Insight. Magnetic Insight. https://www.magneticinsight.com/momentum-imager/. Accessed August 1, 2019.
11. Saritas EU, Goodwill PW, Zhang GZ, Conolly SM. Magnetostimulation limits in magnetic particle imaging. *IEEE Trans Med Imaging*. 2013;32:1600–1610.
12. Schmale I, Gleich B, Schmidt J, et al. Human PNS and SAR study in the frequency range from 24 to 162 kHz. Proceedings of 3rd International Workshop on Magnetic Particle Imaging (IWMPI), Berkeley, CA, USA; 2013. https://doi.org/10.1109/IWMPI.2013.6528346
13. Schmale I, Gleich B, Rahmer J, Bontus C, Schmidt J, Borgert J. MPI safety in the view of MRI safety standards. *IEEE Trans Magn*. 2015;51:1–4.
14. Saritas EU, Goodwill PW, Conolly SM. Effects of pulse duration on magnetostimulation thresholds. *Med Phys*. 2015;42:3005–3012.
15. Demirel OB, Saritas EU. Effects of duty cycle on magnetostimulation thresholds in MPI. *Int J Magn Particle Imaging*. 2017;3:1703010.
16. Yu E, Saritas EU, Conolly SM. Comparison of magnetostimulation limits for axial and transverse drive fields in MPI. Proceedings of 3rd International Workshop on Magnetic Particle Imaging (IWMPI), Berkeley, CA, USA; 2013. https://doi.org/10.1109/IWMPI.2013.6528324
17. Croft LR, Goodwill PW, Konkle JJ, et al. Low drive field amplitude for improved image resolution in magnetic particle imaging. *Med Phys*. 2016;43:424–435.
18. Chronik BA, Ramachandran M. Simple anatomical measurements do not correlate significantly to individual peripheral nerve stimulation thresholds as measured in MRI gradient coils. *J Magn Reson Imaging*. 2003;17:716–721.
19. Harvey PR, Mansfield P. Avoiding peripheral nerve stimulation: gradient waveform criteria for optimum resolution in echo-planar imaging. *Magn Reson Med*. 1994;32:236–241.
20. Dixon WT. Simple proton spectroscopic imaging. *Radiology*. 1984;153:189–194.
21. Fischer MA, Pfirrmann CWA, Espinosa N, Raptis DA, Buck FM. Dixon-based MRI for assessment of muscle-fat content in phantoms, healthy volunteers and patients with achillodynia: comparison to visual assessment of calf muscle quality. *Eur Radiol*. 2014;24:1366–1375.
22. Davids M, Guérin B, Malzacher M, Schad LR, Wald LL. Predicting magnetostimulation thresholds in the peripheral nervous system using realistic body models. *Sci Rep*. 2017;7:5316.
23. Rothman KJ. BMI-related errors in the measurement of obesity. *Int J Obes*. 2008;32:S56–S59.
24. Vogt FM, Ladd ME, Hunold P, et al. Increased time rate of change of gradient fields: effect on peripheral nerve stimulation at clinical MR imaging. *Radiology*. 2004;233:548–554.
25. Ehrhardt JC, Lin C-S, Magnotta VA, Fisher DJ, Yuh WTC. Peripheral nerve stimulation in a whole-body echo-planar imaging system. *J Magn Reson Imaging*. 1997;7:405–409.
26. Lee SK, Mathieu JB, Graziani D, et al. Peripheral nerve stimulation characteristics of an asymmetric head-only gradient coil compatible with a high-channel-count receiver array. *Magn Reson Med*. 2016;76:1939–1950.
27. Zhang B, Yen Y-F, Chronik BA, McKinnon GC, Schaefer DJ, Rutt BK. Peripheral nerve stimulation properties of head and body gradient coils of various sizes. *Magn Reson Med*. 2003;50:50–58.
28. Tan ET, Lee SK, Weavers PT, et al. High slew-rate head-only gradient for improving distortion in echo planar imaging: preliminary experience. *J Magn Reson Imaging*. 2016;44:653–664.
29. Goodrich KC, Hadley JR, Kim SE, et al. Peripheral nerve stimulation measures in a composite gradient system. *Conc Magn Reson Part B*. 2014;44:66–74.